New perspectives in vacuum high voltage insulation. II. Gas desorption

William T. Diamond[a)]
AECL, Chalk River Laboratories, Chalk River, Ontario, Canada K0J 1J0

(Received 5 March 1997; accepted 21 November 1997)

An examination has been made of gas desorption from unbaked electrodes of copper, niobium, aluminum, and titanium subjected to high voltage in vacuum. It has been shown that the gas is composed of water vapor, carbon monoxide, and carbon dioxide, the usual components of vacuum outgassing, plus an increased yield of hydrogen and light hydrocarbons. The gas desorption was driven by anode conditioning as the voltage was increased between the electrodes. The gas is often desorbed as microdischarges—pulses of a few to hundreds of microseconds—and less frequently in a more continuous manner without the obvious pulsed structure characteristic of microdischarge activity. The quantity of gas released was equivalent to many monolayers and consisted mostly of neutral molecules with an ionic component of a few percent. A very significant observation was that the gas desorption was more dependent on the total voltage between the electrodes than on the electric field. It was not triggered by field-emitted electrons but often led to field emission, especially at larger gaps. The study of gas desorption led to some important new observations about the initiation of high-voltage breakdown and the underlying processes of vacuum outgassing. The physical processes that lead to voltage-induced desorption are complex, but there is strong evidence that the microdischarges are the result of an avalanche discharge in a small volume of high-density vapor desorbed from the anode. The source of the vapor may be water or alcohol stored as a fluid in the many small imperfections of a polished metal surface. Microdischarges can then trigger field-emitted electrons which, in turn, heats a small area of the anode. As the temperature of this region of the anode reaches about 500 °C, some fraction of the desorption products are ionized positively and accelerated to the cathode, producing secondary electrons with a yield greater than unity per incident ion. The positive ions appear to originate from the bulk of the metal rather than from surface ionization and the yield increases exponentially with temperature, rapidly producing a runaway condition, i.e., electrical breakdown. These observations support a new perspective on vacuum-high-voltage insulation and produce new insight into vacuum outgassing of metals.
© *1998 American Vacuum Society.* [S0734-2101(98)03102-9]

I. INTRODUCTION

Electrical conductivity and eventual breakdown occurs between two metal electrodes in a vacuum as voltage is increased between them. At least three processes[1] occur that contribute to the conduction: field emission of electrons; transfer of microparticles between electrodes; and microdischarges. In parallel with each of these processes there is an increase in the pressure in the supporting vacuum. In most cases, it is difficult to differentiate cause and effect between the increased pressure and the conduction processes. Microdischarge activity and the associated pressure increase is often the limiting factor in high-voltage devices such as accelerator tubes and electrostatic analyzers.[2] Microdischarges are self-limiting discharges that occur between unconditioned electrodes as the voltage is increased. They can be observed on an insulated anode or cathode as electrical pulses of many microamperes amplitude and hundreds of microseconds width, i.e., about 3×10^9 electrons or ions per microdischarge. The energy dissipated in a microdischarge is much less than the total energy stored by the capacitance of the electrodes. They have often been ascribed to contaminated electrodes[3] or to a regenerative buildup of positive and negative ions. Chatterton[4] (in 1970) provided a good description of the phenomena and gave possible explanations that have not been substantially challenged in the intervening years. His basic argument was that an ionization process is triggered randomly in the gap producing an electron–ion pair, followed by a release of secondary negative ions at the cathode and secondary positive ions at the anode. If ''*A*'' negative ions are produced per positive ion impacting the cathode and ''*B*'' positive ions per negative ion impacting the anode, then if $A\times B$ is greater than unity, the current will grow regeneratively. However, there must be a continual source of new ions at both surfaces. Experiments[5] have been performed to measure the secondary ion coefficients to demonstrate this as a possible mechanism for contaminated surfaces but not clean surfaces under ultrahigh vacuum conditions. There are still many questions about the important phenomenon of microdischarges: for example, the physical processes that occur at one or both electrode surfaces have not been identified; the initiation process is unknown; gas release occurs with a microdischarge but a cause-and-effect relationship has not been established and there have been no attempts to find correlations between microdischarges and vacuum outgassing.

Both this and a companion article[6] report results from an

a)Electronic mail: diamondw@aecl.ca

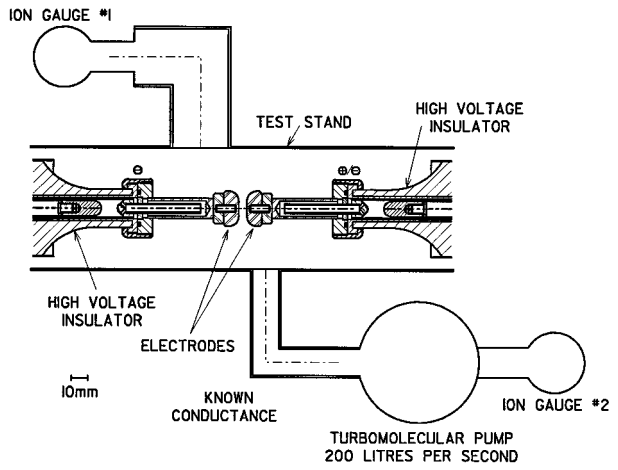

FIG. 1. The experimental setup used for most of the experiments reported in this article. Two high-voltage supplies were used with the polarities shown. The test stand was connected to a turbomolecular pump through a known conductance to measure gas desorption.

extensive research program on vacuum high-voltage insulation. The first article provides strong evidence of physical processes occuring at both electrodes that lead to field emission, a key precursor to electrical breakdown. This article focuses on gas desorption. Evidence is presented suggesting that microdischarges are caused by microbursts of gas of sufficient density to support a local avalanche discharge. The key experiments that support this thesis are described and several new observations are reported. It should be noted that the experiments involve polycrystalline metal surfaces with the inherent imperfections, oxide layers, and other inclusions. It is recognized that the physical properties of such surfaces are very complex. The experimental work has been described in sufficient detail that it can be easily duplicated. The author has presented his interpretation of this data, aware that there may be further explanations.

II. EXPERIMENTAL DETAILS

Most of the experiments reported in this article were done on the test stand shown schematically in Fig. 1. The 10 mm scale shown is indicative of the scale of the vacuum chamber, insulators, and electrodes. The ion gauge and pumping connection are shown schematically. The test stand was the same used for experiments reported in the companion article.[6] Throughout the research program, many different configurations were used for specific experiments. The author has chosen to show significant modifications to the basic test stand with specific experimental results to highlight the changes.

Details of the high-voltage insulators and the high-purity water system used to provide cooling plus a series surge resistance are provided elsewhere.[7,8] Two variable high-voltage power supplies were used, one with a maximum rating of -100 kV, and the other with a maximum rating of ± 150 kV. The cable insulation and the ceramic insulator limited the maximum useable voltage to about 110 kV. In order to study gas desorption, the test stand was configured with two ion gauges, which together with the known conductance between the test volume and the 200 ℓ/s turbomolecular pump, allowed mass flow to be calibrated. A residual gas analyzer was used for some measurements. It was mounted near the pump for most experiments. Other configurations were used including one high-voltage supply and a grounded second electrode.

Typical base pressures in the test stand were $2-10 \times 10^{-7}$ Torr depending on pumpdown times. For most experiments, unbaked electrodes, 12 mm thick$\times$25 mm diameter and radiused as shown, were used. Oxygen-free copper, niobium, titanium, and aluminum electrodes were tested. The usual surface preparation was either electropolishing or micropolishing of both electrodes. Micropolishing means successive polishing of machined electrodes with wet aluminum-oxide papers to 600 grit, polishing with 1/2 μm aluminum oxide suspended in water on a low-lint wipe, and finishing with either a submicron silicon oxide polish in a basic (pH$=9$) solution or commercially available Brasso® (pH$=10$) polish. The interior of the test stand was also finished in a similar manner. With these surface preparations, very high electric fields could be reached before any measurable field emission occurred[6] and tests of gas desorption phenomena could be made independent of competing effects from field emission.

X-ray activity was measured during many experiments with several radiation-survey instruments, scintillation detectors and a high-quality silicon detector. The scintillation detectors provided sensitive temporal response to x-rays while the geiger counter provided high x-ray sensitivity to cw field emission. It could measure an increase in x-rays above background that corresponded to measured electron currents of about 50 pA at 50 kV and less than 20 pA at 100 kV.

III. EXPERIMENTAL RESULTS

A. Microdischarges and gas desorption

1. Properties of a microdischarge

Microdischarges typically occur when dc voltage is increased between two unconditioned electrodes. There is initially no measurable electrical activity, then at some voltage electrical conduction begins between the two electrodes. In a typical experiment reported in this article, the voltage was increased between two well-polished electrodes at gaps from 1 to 10 mm. At about 40–60 kV, the pressure in the test stand increased strongly and microdischarges were observed. In periods of seconds to minutes the microdischarge activity and conduction between the electrodes decreased and with time constants of minutes to tens of minutes, there was no measurable electrical activity in the gap between the electrodes. When the voltage was increased from this conditioned level, microdischarge activity immediately increased again in both frequency and amplitude, with a corresponding increase of pressure in the test stand. At small (1–2 mm)

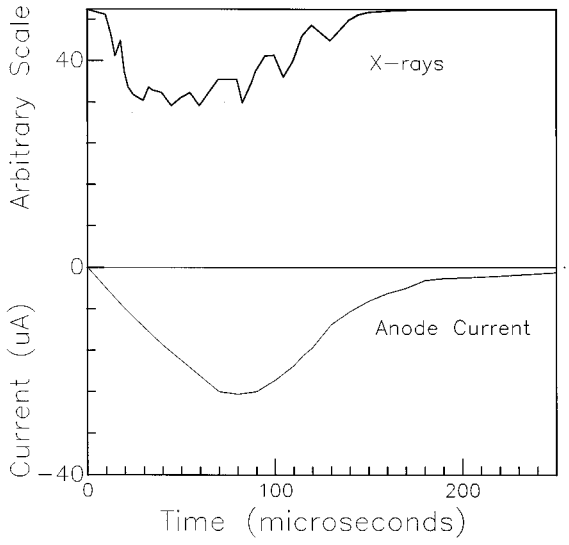

FIG. 2. Some properties of a typical microdischarge. The upper trace shows x-ray production during the microdischarge while the lower trace shows the current collected on an insulated anode connected to ground with a 1 kΩ resistor.

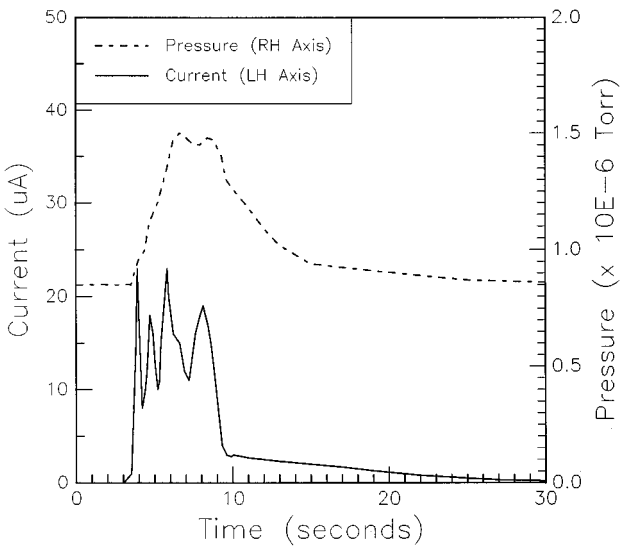

FIG. 3. The pressure rise (upper trace) and current produced as the voltage was increased from 60 to 70 kV between two copper electrodes with a 3 mm gap.

gaps, a transition to field emission eventually occurred. At larger gaps, 100 kV could be maintained for several days with no observable electrical activity.

Figure 2 shows some properties of a typical microdischarge occurring between two copper electrodes at a gap of 2.5 mm and 60 kV. This figure shows the anode current (lower curve) and the x-ray activity (upper curve) as a function of time. In these experiments a negative high-voltage supply was used and the anode was mounted on an insulated electrode holder that was grounded through a 1 $k\Omega$ resistor. For this geometry, the amplitude of the current pulses varied from a few to 50 μA, increasing when the voltage was increased and decreasing as conditioning occurred while maintaining a pulse width variation of about a factor of 2. Over a wider range of experimental conditions, the peak current during a microdischarge varied from a few to 500 μA and the pulse width from about 50 to 500 μs.

The x rays were measured with a small cesium iodide detector viewing the electrodes through a glass window at a distance of 10 cm. The x-ray response demonstrated considerable pileup during the microdischarge and did not faithfully mirror the time response of the anode current. If the detector was pulled back from the window, the x-ray signal reflected the time response more accurately but there was not sufficient sensitivity to measure x rays that might have been present during the period between microdischarges. Microdischarges can be present with or without simultaneous field emission. Many measurements were made in which there was no measurable x-ray activity present either before or after the microdischarge. This has been interpreted[9] as an indicator that field-emitted electrons are not a precursor to the microdischarge. It was not possible to distinguish from this data whether the x rays produced during the microdischarge were from field emission, electrons produced in the gap in an avalanche discharge, or from electrons produced at the cathode purely as secondary emission from positive-ion bombardment. Figure 2 shows some of the properties of microdischarges but does not help elucidate the mechanisms of production.

Figure 3 demonstrates another aspect of microdischarge activity. The upper half of the figure shows the change of pressure in the test stand observed after an increase of 10 kV during the time from 4 to 8 s (from 60 to 70 kV over a 3 mm gap with 1.9 cm diameter copper electrodes); the lower half shows the current measured on an insulated anode grounded through 1 kΩ. The pressure rise corresponded to a dramatic increase in the number of microdischarges similar to those shown in Fig. 2 but with some variation in amplitude with time. The peak increase in pressure corresponded to microdischarge rates of about 1–2 kHz, dropping to less than 100 Hz by 30 s and to less than 1 Hz after a few minutes. The rate was determined by measuring, with an oscilloscope, the number of individual microdischarges in a 0.1 s interval at various times after the voltage was increased, and has considerable variation in different measurements. Once the microdischarge activity stopped there was no measurable x-ray activity above background.

2. Quantity of gas released

The data of Fig. 3 can be used to measure the quantity of gas released following the voltage increase. The integral of the pressure–time curve (about 3.6×10^{-6} Torr s) multiplied by the pumping speed of the chamber through the calculated conductance (70 ℓ/s) gives the total gas released (Torr ℓ). For Fig. 3, that number is about 2.5×10^{-4} Torr ℓ, a large quantity of gas. Most of the gas was desorbed during approximately 5 s and if it were desorbed only from the center portion of the electrodes of about 3 cm^2 area each, then the

desorption rate would be about 1.6 or 0.8 $\times 10^{-5}$ Torr ℓ/s cm^2, depending on whether the gas was desorbed from one or both electrodes. This corresponds to 9 $\times 10^{15}$ molecules, equivalent to several monolayers (about 10^{15} molecules/cm^2 per monolayer) if the gas originated from the electrode surfaces. However, the gas could also be produced from any part of the test stand or insulator.

The lower curve shows the current from the high-voltage power supply during the gas desorption. This nominal cw current is made up of the sum of all the individual microdischarges. At the peak current, the microdischarge rate was about 2 kHz; the pulse duration 200 μs and the pulse current about 20–30 μA. This produces the nominal 8–10 μA cw current for 5 s as shown in Fig. 3. Approximately 10 000 microdischarges produce about 10^{16} molecules, implying that each individual microdischarge contains around 10^{12} molecules. The integral of the current over time is about 4 $\times 10^{14}$ ions or electrons, a few percent of the number of neutral molecules.

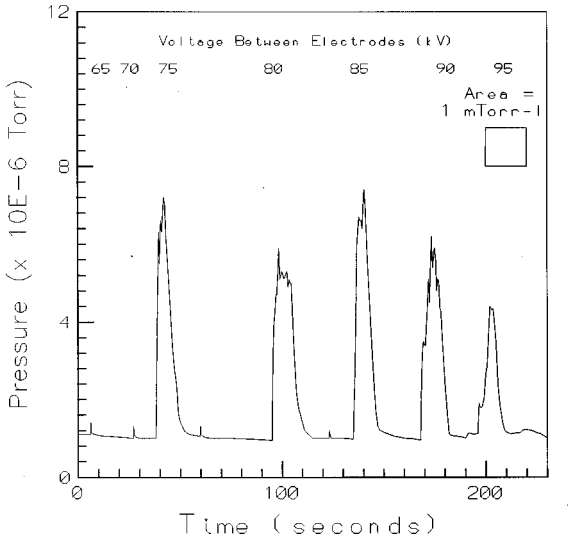

FIG. 4. Test stand pressure vs time as the voltage was increased between titanium electrodes at a 4 mm gap. The upper line of data shows the voltage difference between the electrodes as one power supply was turned down. The rectangular insert shows the graphical area equivalent to 1 mTorr ℓ of desorbed gas.

B. Gas desorption experiments

1. Experiments to identify the source of the desorption

The data in Fig. 3 give an estimate of the total gas desorbed after an increase in voltage. However, the gas may have been desorbed from many different locations. The experimental setup shown in Fig. 1 was used to measure the amount of gas desorbed only from the electrodes. Micropolished titanium electrodes, 25 mm diameter, were mounted on both insulators and positioned at a gap of 4 mm. The two power supplies were both used with negative polarities and the voltage of both was slowly increased to -100 kV with the relative voltage between the electrodes at less than 10 kV. Gas could be desorbed from various sources during this conditioning process, including the test stand and the insulators. After about 20 min there was no indication of further desorption, as observed by quiescent vacuum and the lack of x-ray production. The voltage on one of the power supplies was then decreased in increments of 5 kV while the other was left at high voltage. This technique (referred to as a ''double negative'' experiment elsewhere in this article) ensured that the only increasing electric field was that between the two unconditioned electrode surfaces. Once gas evolution was observed, the voltage was maintained at a fixed value for about a minute after each 5 kV change while the pressure of both ion gauges was recorded with a strip chart recorder. Figure 4 shows the results of this measurement. The x axis shows the time as measured by the recorder and the y axis shows the pressure in the test stand. The voltage difference between the electrodes is shown above the data. The test stand pressure increased dramatically after each 5 kV increment and decreased in about 15 s to near the starting pressure. Other experiments demonstrated that if this same rapid increase in voltage was applied at a smaller gap such as 2 mm, it was likely to lead to a spark and the transition to field emission. For this particular data, there was no measurable x-ray yield after about 10 min with 95 kV between the electrodes.

The insert on the upper right part of Fig. 4 shows the area that corresponds to 1 mTorr ℓ of gas desorbed from the electrodes. If the area corresponding to the pressure increases is integrated, an estimate of the gas desorbed versus the voltage difference can be made. This is shown in Fig. 5. The y axis shows the differential gas desorption, i.e., the gas desorbed per 5 kV increment, with the data points plotted for the

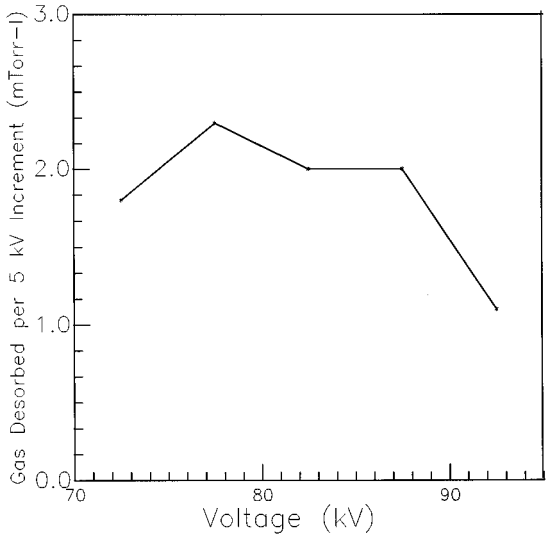

FIG. 5. The differential gas desorption from the data of Fig. 4. Each data point corresponds to the area of a peak in the pressure–time graph for a 5 kV increment. The points are plotted for the average voltage of the increment and the line merely joins the points.

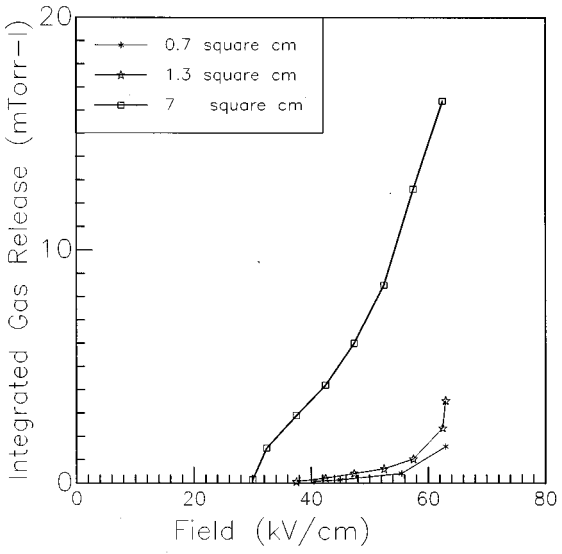

FIG. 6. The integrated gas desorbed from three sets of copper electrodes of different areas vs voltage for a gap of 1.5 mm.

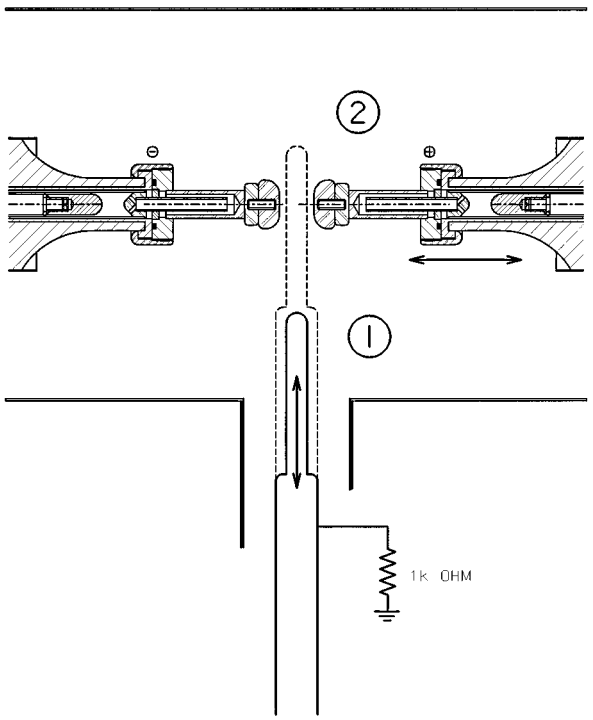

FIG. 7. Experimental setup to test desorption from an unconditioned electrode opposite a conditioned electrode.

average voltage of a given increment. Figure 6 shows the results of similar experiments with polished copper electrodes of three different areas at a gap of 1.5 mm. The *y* axis is, in this case, the integral of the gas released as a function of the voltage. The listed areas are quite approximate because the same radiused edge ($\sim$6 mm radius) was used for all three electrodes and the radiused region is subject to different fields than is the flat region. Within these approximations, the gas released per unit area from each experiment in Fig. 6 was approximately the same, 2.3 mTorr ℓ/cm^2, or 8 $\times 10^{16}$ molecules/cm^2 at 80 kV or half of this value if the gas were desorbed from both electrodes. Similar results were found for all metals tested: aluminum, copper, titanium, and niobium.

Several experiments were performed to crosscheck these results. Since electrons and ions were also produced, there was concern that these charged particles could lead to changes in the ion gauge readings. To test this, a pumping restriction was placed between the turbomolecular pump and the roughing pump. The pressure rise at the entrance to this restriction was measured with a thermocouple gauge when a pressure rise from gas desorption was observed with the ion gauges. The system was calibrated by bleeding air into the test stand and recording the pressures measured by the two ion gauges and the thermocouple gauge as the test stand pressure was increased by two orders of magnitude. Within about 25%, this independent measurement using a completely different physical principle to measure the pressure increase confirmed the results shown in Figs. 5 and 6. The thermocouple gauge indicated a lower throughput than the ion gauges. However, it has a longer time constant than the ion gauges, and may not have reached equilibrium during the few seconds of peak microdischarge activity. It should also be noted that the gas desorption results have not been corrected for the gas composition, which had a higher concentration of light hydrocarbons, carbon dioxide, and carbon monoxide than would be typical at this pressure.

A second confirmation that the indicated pressure increases were real and not induced by the charged particles was the discrimination of a residual gas analyzer (RGA) to individual peaks. The data is considered in detail in Sec. III E. However, it is noted that if the changes in ion gauge readings were produced by the electrons and ions from the desorbed gas, the RGA should not exhibit the sharp discrimination.

2. The precursor of gas desorption

The experiments described in Secs. III A and III B 1 demonstrated the production of large quantities of gas from the electrodes during the high-voltage conditioning process. Experiments were then designed to try to understand what initiated the desorption. Figure 7 shows one experimental setup used. Micropolished copper electrodes were mounted on both high-voltage electrodes with the polarities shown. A third electrode was mounted on a movable, insulated tube on the side of the test stand that was grounded through 1 kΩ. This electrode was made from oxygen-free copper with the same micropolished surface preparation used for the two inline electrodes. The side-mounted electrode was moved to position 1 while the two inline electrodes were conditioned to high voltage. Each electrode and insulator was conditioned to 100 kV and operated there for 20 min with the other electrode at zero volts at a gap of 3 mm. No field emission was detected during this process. The positive elec-

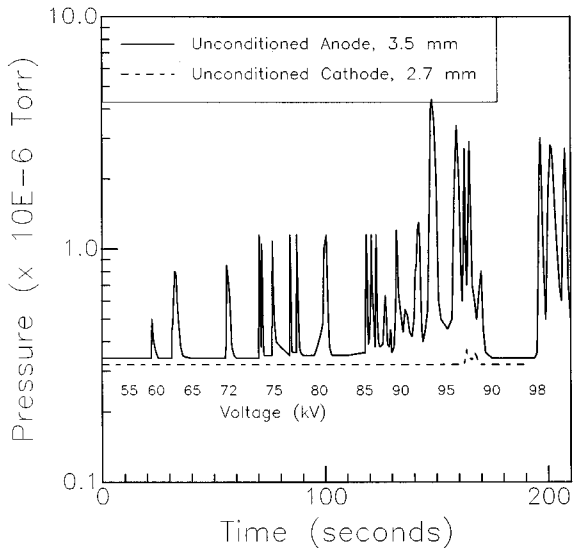

FIG. 8. Results from increasing the voltage between an unconditioned anode and a conditioned cathode (solid line) and an unconditioned cathode and a conditioned anode (dashed line). The actual voltage is shown below the data.

trode was then moved back to a predetermined position such that a gap of 2.7 mm (measured after the conclusion of the experiment to avoid electrode contact before data was taken) would exist between it and the side-mounted electrode once it was moved into position 2. The positive high-voltage electrode was reconditioned to 100 kV in this location before the side-mounted electrode was moved into position 2. These procedures were designed to ensure that gas desorbed during the next phase of the experiment would come only from the side-mounted electrode. This electrode was then moved into position 2 with a gap of 3.5 mm between the well-conditioned cathode electrode and an unconditioned anode surface, and a gap of 2.7 mm between a well-conditioned anode electrode and an unconditioned cathode surface. High-voltage was applied with one power supply while the other was left at zero volts. Power supply current and test stand pressure were monitored during this process.

Figure 8 shows the results of the changes in pressure as the voltage was increased in two different experiments. The data were recorded on a strip chart recorder and the *x* axis is a measure of time. The numbers above the *x* axis indicate the voltage used at a given time. The *y* axis shows the pressure in the test stand. The dashed line shows the results for an unconditioned cathode and a conditioned anode. Clearly, there is no change in pressure throughout the entire process until the voltage reaches 95 kV at which point some desorption occurs. A field of 35 MV/m was reached in under 200 s with no indication of gas desorption or any other conditioning activity.

The solid line shows the data when the cathode was previously conditioned and the anode was unconditioned. This data is similar to that shown in Fig. 4. Large quantities of gas were desorbed at each increment starting from about 55 kV over a 3.5 mm gap. The voltage was decreased slightly at 175 s and the conditioning activity stopped until the voltage was turned up to the previous level of conditioning. This demonstrates that the conditioning activity is driven by the anode. The gas could be desorbed from either electrode because there is also ionic bombardment of the cathode. Figure 8 demonstrates that high-voltage conditioning of well-polished electrodes occurs mainly at the anode surface, a surprising result.

This experiment also demonstrates that the product of the secondary emission coefficients ''*A*''×''*B*'' being greater than unity is not the complete explanation of microdischarge activity because conditioning one electrode should alter one of the coefficients. The conditioned cathode had no measurable field emission at 100 kV over 3 mm, with a detection sensitivity of about 20 pA. Since field-emitted current increases rapidly with field, any possible undetected field emission would be below the picoampere level at the first stages of gas desorption. It is therefore unlikely that field emission is the precursor to gas desorption. Experiments described in Sec. III D using larger gaps also produced this same observation.

A second experiment demonstrated that thermal desorption of an anode also conditions it. An unconditioned, micropolished copper anode was heated with electron bombardment to about 700 °C, cooled, and moved into position at 2.5 mm from a cathode mounted on the high-voltage insulator. The cathode had previously been conditioned to 100 kV over 3 mm with a different anode mounted from the side port. When the thermally desorbed anode was tested, there was essentially no desorption as the voltage was increased to 100 kV. The chamber was then vented with dry nitrogen, repumped, and high voltage was applied again with little desorption seen during the test. The chamber was vented again, the anode wiped with ethanol, and the chamber repumped. Some desorption was observed as the high voltage was increased again, although less than during the first experiment.

C. Dynamics of a gas discharge

In Sec. III A it was speculated that a microdischarge was a burst of gas with sufficient density to maintain an avalanche discharge for a short time. Section III B showed measurements of the quantities of gas desorbed. In this section, several experiments are described that were designed to study the dynamics of an avalanche discharge in the same geometry. Figure 9 shows the simple experimental setup used. Gas (usually air or nitrogen) flowed through a 0.5 mm diameter hole in the center of one copper electrode. The other electrode was mounted on a standard high-voltage insulator and could be used as either an anode or cathode. Gas flow was monitored by measuring the pressure in both the test stand and above the turbomolecular pump with a known conductance between them. A specific voltage was set and the gas flow was increased until current was conducted.

When the electrode with a hole was a cathode, it was observed that the onset of electrical activity was very unstable, somewhat like a spark in which tens of milliamps

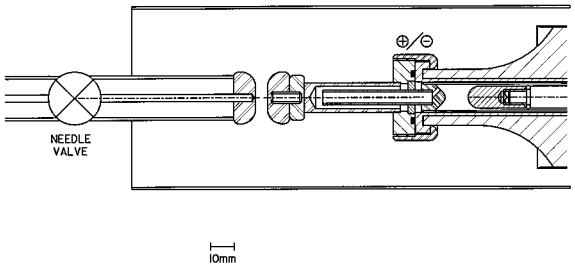

FIG. 9. Experimental setup used to measure an electrical discharge between two electrodes with the same geometry as in the high-voltage tests. Various gases were flowed through a 1/2 mm hole in the grounded electrode while the other electrode could be either a cathode or anode.

were conducted. The onset rapidly quenched in about 10 μs, and repeated as soon as the voltage had recharged through the $\sim 25\ \mathrm{M}\Omega$ series resistance provided by the water resistor.

When the electrode with a hole was an anode, a stable discharge occurred. Figure 10 shows some typical results of current versus test stand pressure for a 2 mm gap and voltages of 10, 20, and 30 kV. The current increased exponentially with gas throughput for a fixed gap and voltage. The current also increased exponentially with voltage for a fixed gap and gas throughput.

Trial 3 provides a typical example for comparison with a microdischarge. At 30 kV and a pressure of 3.5×10^{-4} Torr, there is a current of 60 μA. The throughput is 2.5×10^{-2} Torr l/s$=8\times10^{17}$ molecules/s, or 8×10^{11} molecules/μs. In 50 μs, equivalent to a microdischarge, there would be 4×10^{13} molecules in a visible discharge of somewhat greater than the 1/2 mm diameter hole. This is of similar order of magnitude to the estimated 1×10^{12} molecules in a microdischarge (see Sec. III A). It is not known what the diameter of the microdischarge might be but it is likely to be much smaller than 1/2 mm. The gas density in a smaller

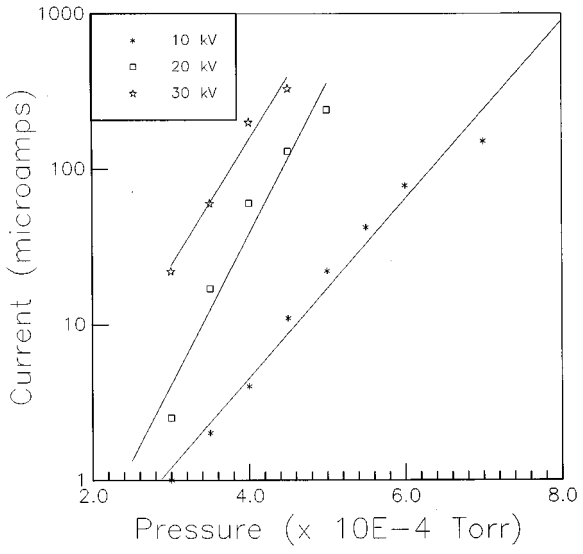

FIG. 10. The results of tests with air flowing through the hole in an anode. Data is shown for three different voltages and a gap of 2 mm.

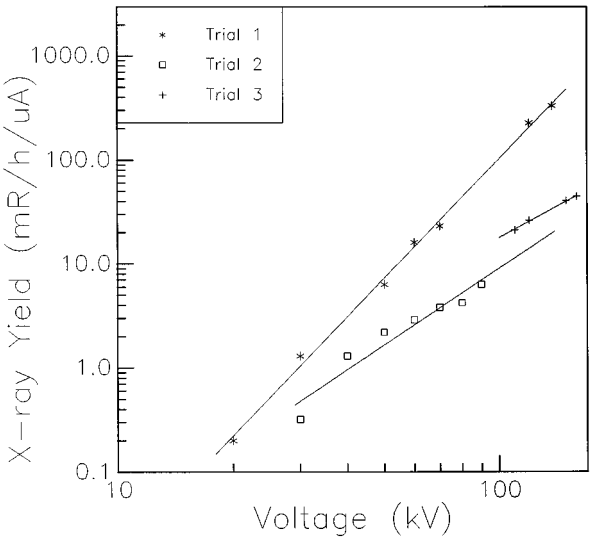

FIG. 11. A comparison of the x-radiation produced between two copper electrodes at a gap of 3 mm during field emission (trial 1), nitrogen gas flowing through a 1/2 mm hole in the anode (trial 2) and during gas desorption as high voltage is increased (trial 3). The data for trial 3 was taken immediately after increasing the voltage to the value indicated by the data point. The time constant of the radiation detector was significantly faster than the 5–10 s that the radiation yield remained nearly constant.

volume could readily reach that required for an avalanche discharge. It is noted that there is no electrical activity if this experiment was conducted by bleeding the gas from a side port until pressures of greater than 10^{-3} Torr were reached.

Another interesting test of whether microdischarge activity is produced by an avalanche discharge in a local high-pressure gas burst is by observing x-ray production. Figure 11 shows the results of measurements of radiation made using a health-physics ionization chamber placed at the glass window, viewing the electrodes. This figure shows the radiation produced per μA of current conducted between two copper electrodes versus voltage, for several different processes. Trial 1 shows the x-ray yield for field emission versus the voltage between the electrodes. Field-emitted electrons would be produced at the cathode and gain the full energy of the power supply before impacting the anode. Trial 2 shows the radiation produced when nitrogen gas was flowing through a hole in the anode, as shown in Fig. 9. In this case, electrons are produced throughout the volume but most are not accelerated through the full potential of the gap. This results in a much lower yield of lower energy x rays. The x-ray yield varied, depending on the length of the gap; the data for trial 2 was for the same gap (3 mm) as used in trial 1. Trial 3 shows the radiation produced during microdischarge activity at a 3 mm gap. The x-ray yield for this case is clearly much closer to that produced for a gas discharge than for a field-emitted electron beam. There was no opportunity to use electron suppression for any of these experiments and current measurements may have significant errors because of secondary processes; however, these effects are likely to be similar for all three experiments. With this proviso, these data show consistency with the picture of microdischarges as

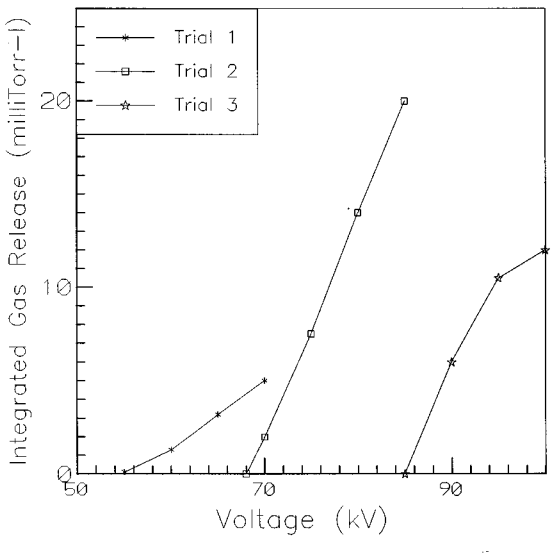

FIG. 12. Demonstration that high-voltage-induced gas desorption depends more on the voltage than the field. Trial 1 shows the integral of the gas desorbed in a double-negative experiment with copper electrodes at 2 mm. Trial 2 shows the integral of gas released with increasing voltage at a 10 mm gap and trial 3 at a 15 mm gap.

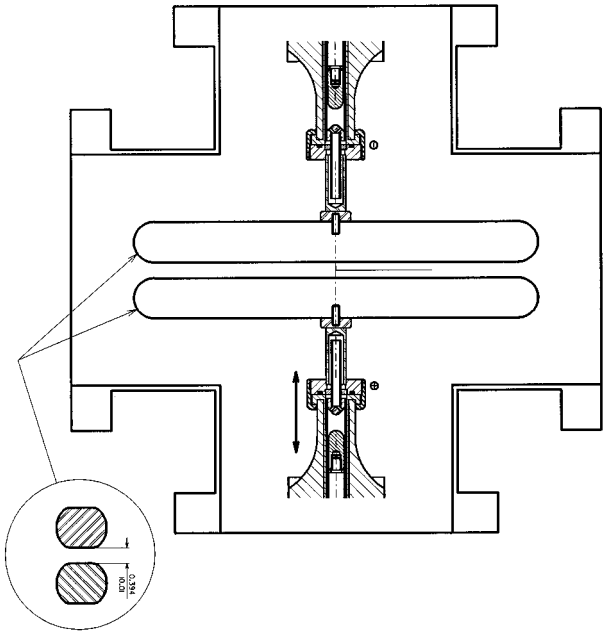

FIG. 13. Experimental setup used to demonstrate the transition to field emission during gas desorption. Aluminum electrodes, 25 cm long by 3 cm high, were tested at voltages up to +/−100 kV over a 1 cm gap.

avalanche discharges in gas desorbed from the anode in discrete bursts.

D. Total voltage effect

1. Gas desorption-voltage dependence

Many experiments were conducted that demonstrated gas desorption. One very interesting observation was that gas desorption seemed to have a much stronger dependence on the total voltage than on the electric field. The data of Figs. 5 and 6 provide an indication of this. The amount of gas desorbed was similar for the same electrode area and voltage, even though the gap was 4 and 1.5 mm for Figs. 5 and 6, respectively. Figure 12 shows the results of an experiment that demonstrated that gas desorption was largely dependent on the total voltage. Two 36 mm diameter micropolished copper electrodes were used in a double-negative (see Sec. III B 2) experiment. In this experiment, the two electrodes were conditioned together to 100 kV at a gap of 2 mm. The voltage of one electrode was reduced in 5 kV increments until gas desorption was measured, starting at 55 kV difference. Trial 1 shows the integral of the gas desorbed as the voltage difference was increased to 70 kV. The voltage was then equalized at 100 kV, the gap was increased to 10 mm, and the process repeated. Trial 2 shows that gas desorption began again at about 70 kV and increased strongly until the trial was stopped at 85 kV. Each trial shows only the integral of gas desorbed for that test. The process was repeated and the gap set to 15 mm. Trial 3 shows that gas desorption began again about 85 kV and continued until the maximum voltage difference of 100 kV was reached. This experiment provided another strong indication that field-emitted electrons are not part of the process because the microscopic field at the cathode was reduced by a large factor, and there was no measurable field emission at any time during the experiment.

2. Transition to field emission

Our previous work has shown[6] that the transition to field emission can occur via several processes. In one process, microparticles can be pulled from the anode to the cathode, providing both a potentially rougher site on the cathode with higher field enhancement and an area of reduced work function. Alternately, small areas of the cathode can be removed, producing the same effect. Once field emission is present, thermal instabilities in the anode contribute to eventual breakdown. The transition to field emission at larger gaps and lower fields is a key aspect of this process because if there were no field-emitted electrons, anode-initiated breakdown would not be possible except through the transfer of microparticles. It has been observed during many experiments that the transition to field emission can occur during microdischarge activity and the attendant pressure rise. This may be the dominant limiting effect in reaching high fields at large gaps.

Figure 13 shows an experiment to measure high-voltage standoff for electrodes with much larger area than used for the other experiments reported in this article. The electrodes were made from AA2024 aluminum with the cross section shown, a length of 25 cm and a gap of 1 cm. The test stand was a standard 15 cm diameter vacuum cross that had been moderately polished; it was not possible to reach the high-quality polish of the test stand on a surface that had not been machined. The electrodes could be used at positive and nega-

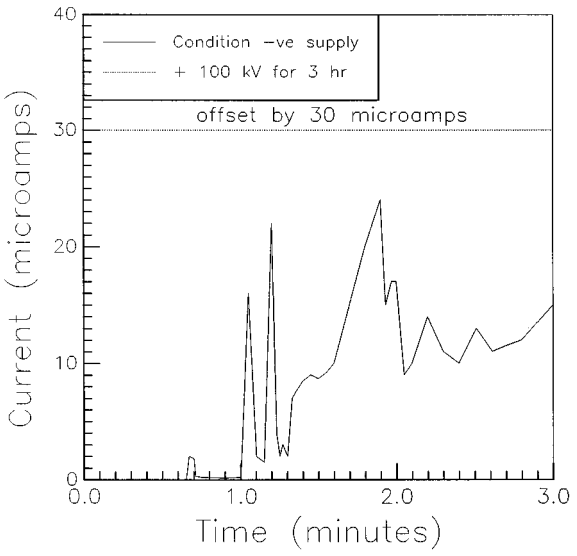

FIG. 14. High-voltage conditioning of each electrode. The dashed line shows operation of the anode at 100 kV with respect to the chamber and the opposing electrode (at 1 cm) for 3 h after initial conditioning. The solid line shows the conditioning process for the cathode. The two sparks at about 1 min represent a transition to field emission.

tive 100 kV as shown. The positive electrode was initially conditioned to 100 kV with the negative electrode at 0 V. Gas was desorbed from this electrode during the conditioning process and then stable operation was achieved. Figure 14 shows results from this experiment. The dashed line shows the power supply current measured with the strip chart recorder while the positive electrode was tested at 100 kV for 3 h with the negative supply at 0 V. There was no electrical activity observed. The positive supply was then set to 10 kV and the negative supply was increased. The solid line shows the current measured during this process over 3 min rather than 3 h as shown by the dashed line. At -60 kV, there was a large increase in pressure (not shown) and current was measured between the two electrodes as usually occurs during gas desorption. The two sharp increments are indicative of small sparks. When the pressure restabilized, there were still field-emitted electrons flowing between the electrodes, at a field of only 70 kV/cm. This occurred despite the fact that the electrodes had operated at 100 kV/cm for 3 h with no field emission, as shown by the dashed line in Fig. 14. The gas must have been desorbed from the vacuum chamber rather than from the nearby anode which had already been conditioned. The vacuum chamber was an anode when the negative electrode was conditioned but a cathode when the positive electrode was conditioned. The transition to field emission occurred during the gas desorption but field emission may have been produced from the transfer of a microparticle from the chamber surface to the cathode.

The cathode was then repolished, the vacuum chamber wiped with alcohol and the experiment repeated. Once the cathode was successfully conditioned to 100 kV, the two electrodes were then conditioned to 180 kV over a 1 cm gap. The electrodes were operated at 180 kV/cm for two days with no field emission or other indicator of electrical activity throughout this period. At that time a small spark occurred and field emission was present.

This experiment demonstrated a practical aspect for high-voltage devices, namely, to use the minimum anode area that is practical and use the chamber as a cathode. However, all the cathode area must then be polished or else sharp projections on its surface can serve as a source of field emission.

E. Gas desorption processes

The physical processes that lead to high-voltage-induced gas desorption are not well understood. An important question arises—is the amount of gas desorbed as the voltage increases representative of the quantity and composition of the gas that is present in a polished metal surface.[2] In general, gas can be desorbed from metal surfaces in a high vacuum by several processes,[10] including vacuum outgassing, thermal-induced desorption, and photon or electron-impact desorption. Vacuum outgassing is a process that occurs as soon as any material is placed in a vacuum and is dominated by desorption of water vapor that has been adsorbed into the surface. An experiment has been performed[11] that measured, with secondary ion mass spectrometry, the penetration of ^{18}O from $H_2{}^{18}O$ (to differentiate it from other oxygen) into a metal surface. A concentration of a few tenths of a percent of water molecules still persisted at depths beyond 100 atomic layers. There is also a large concentration of carbon on most metal surfaces.[12]

The vacuum outgassing (desorption) rate is given by

$$Q(t) = Q(t_0) \times 1/t^n,$$

where $Q(t_0)$ is the outgassing rate at some defined starting time such as 1 h, and n varies from 0.7 to 2 but is typically near unity. The outgassing rate of many metal surfaces can vary from 10^{-7} to 10^{-12} Torr ℓ/s cm^2 or less, depending on surface preparations, type of metal, and time after pumpdown. This is at least several decades less than the observed rate (about 10^{-5}) reported in Sec. III A 2 for gas desorbed under the influence of increasing high voltage.

When metal is heated in a vacuum, the outgassing rate increases substantially because of thermal-induced desorption and the spectral composition of the products changes as the temperature is increased.[13] The total quantity of gas desorbed is often much greater than a single monolayer ($\sim 10^{15}$/cm^2) for outgassing either at room temperature or elevated temperatures. It is noted that an average outgassing rate of 5×10^{-8} Torr ℓ/cm^2/s for 1 h represents a loss of 6×10^{15} molecules/cm^2, equivalent to about six monolayers. This is typical of outgassing rates of many metals measured soon after pumpdown. One explanation[14] of the large quantities of desorbed material is that the apparent area of the metal is much greater than the geometric area because of surface irregularities. The material is adsorbed at monolayer depths over this larger area.

Experiments were performed in the test stand to measure thermal desorption from the micropolished 25 mm diameter electrodes used in the high-voltage experiments. Niobium,

TABLE I. The quantity (mTorr ℓ) of gas desorbed from the micropolished electrodes listed as the temperature was increased. The data shows the integrated gas released for the temperature listed.

Temperature °C	Cu	SS	Al	Nb	Ti
100	0	1	2.8	0.5	1.5
150	0.6	2	5	1	4
200	1.6	3	8	2	7
250	3	4	11	3.5	12
300	5	5	14	5	14
350	8	6	16	8	20
400	10	9	20	12	25

copper, aluminum, stainless steel, and titanium electrodes were tested. An electrode was heated on a thin stainless steel tube with a cartridge heater, mounted in air, that heated the end of the tube and the electrode sample. The tube was first heated to 600 °C without an electrode in place, while the pressure was recorded with both ion gauges (see Fig. 1), and a RGA was used to measure gas composition. The test stand was vented with helium, a micropolished electrode was then mounted, and the process was repeated. Table I shows the integral of the gas desorbed from each 25 mm diameter electrode as a function of temperature.

There was about 20% more gas released during the return to room temperature while the typical background from reheating an electrode without venting the test stand was about 5%. If the test stand was vented, the electrode removed to air for 30 s, reinstalled and heated through the same thermal cycle, the gas release was 10%–15% of that shown in Table I. The area of the electrodes was approximately 15 cm^2. Therefore, the total gas released was 1–2 mTorr ℓ/cm^2 equivalent to about 5×10^{16} molecules/cm^2, similar to that reported in Sec. III A 2 for gas released from high-voltage desorption.

An experiment was then done in which two large (3.8 cm diameter) copper electrodes were repolished and the anode mounted on the stainless-steel tube used for the thermal desorption experiments. Gas was desorbed by increasing high voltage up to 90 kV over a 3 mm gap. The quantity of gas desorbed was similar to that measured with the same electrodes in the experiment reported in Fig. 6, about 17 mTorr ℓ. The high voltage was turned off and the electrode was heated to about 500 °C. The total quantity of gas desorbed during this half of the experiment was about 13 mTorr ℓ. The area of the electrode is about 35 cm^2. It appears that the increasing high voltage had efficiently removed a substantial fraction of the adsorbed material on the front side of the electrode.

The composition of the desorbed gas was measured with a RGA as the voltage was increased between two copper electrodes, for comparison with the composition from thermal desorption. The RGA could monitor up to eight individual peaks as a function of time. Figure 15 shows the results of heating a micropolished copper electrode during the tests reported in Table I. The *x* axis is temperature and the *y* axis shows the partial pressure of mass 2, 18, 28, 32, and 44.

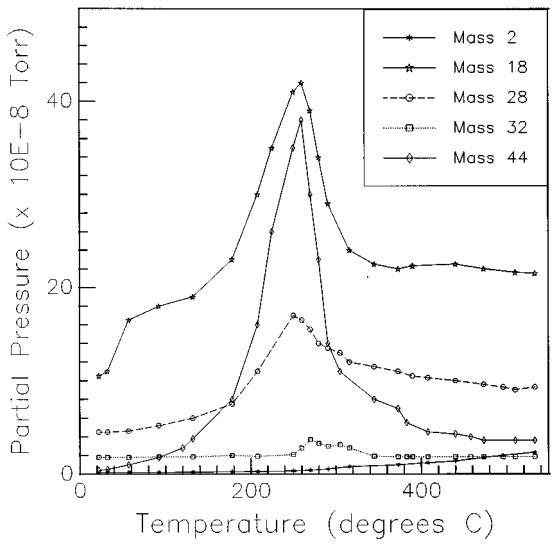

FIG. 15. The partial pressure of masses 2, 18, 28, 32, and 44 as a function of temperature as a micropolished copper electrode was heated from room temperature to 550 °C.

Three other peaks (mass 12, 55, 64), contributing less than a few percent of the total pressure, were also monitored. Figures 16 and 17 show the results of increasing the voltage between 36 mm diameter micropolished copper electrodes. The *x* axis shows time and the *y* axis shows the partial pressure of masses 18, 28, and 44 (Fig. 16) and masses 2, 15, and 32 (Fig. 17). The voltage was increased from about 60 to 75 kV during the time from 0.3 to 1.2 min while attempting to maintain a reasonably steady pressure increase during that period. The fluctuations represent unavoidable pressure changes during the sampling. The tests were performed soon after pumpdown of the test stand, and water vapor was the

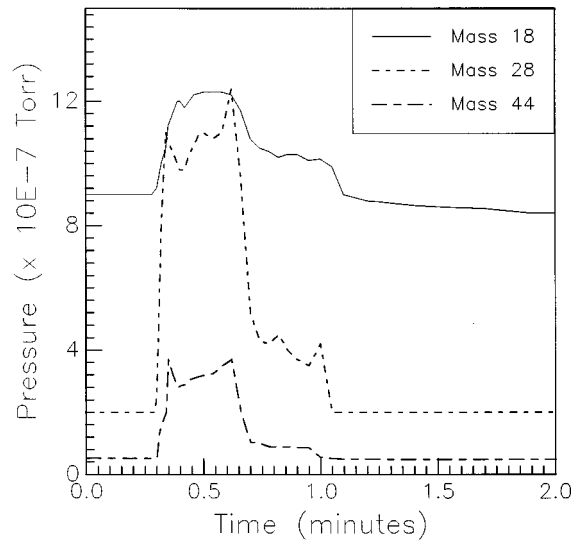

FIG. 16. The partial pressure of masses 18, 28, and 44 as the voltage was increased between 36 mm diameter, unconditioned, micropolished copper electrodes at a gap of 5 mm.

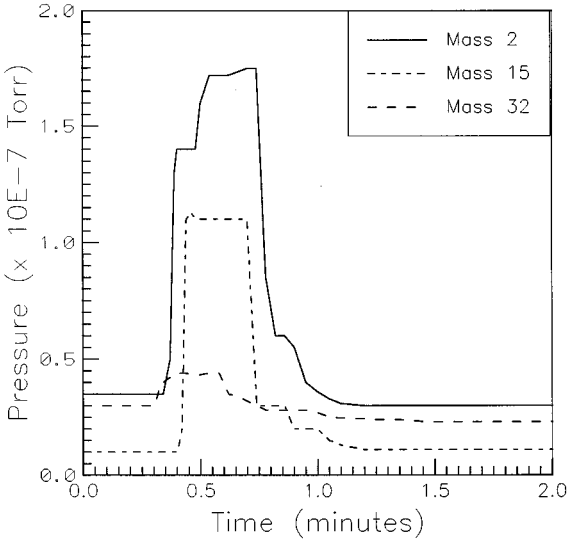

FIG. 17. The partial pressure of masses 2, 15, and 32 for the same conditions as in Fig. 16.

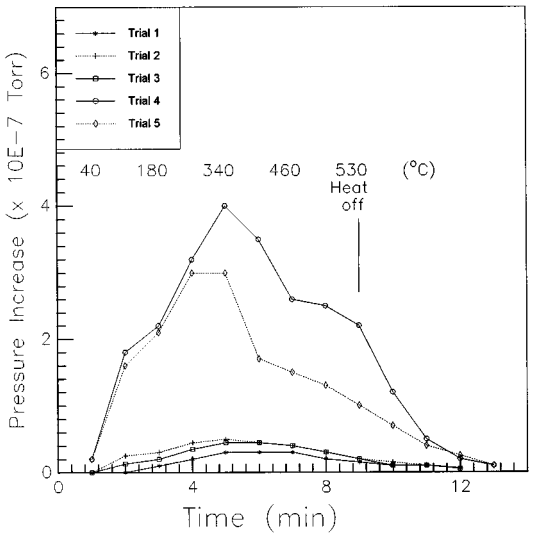

FIG. 18. The gas desorbed from a heated stainless-steel tube as it was heated through a thermal cycle to 540 °C and cooled to near room temperature. The different trials are explained in the text.

dominant peak before the gas desorption occurred. The absolute change in this peak was significant but the fractional change was only about 1.4, similar to the fractional change in oxygen, while the fractional change in hydrogen, light hydrocarbons, carbon monoxide, and carbon dioxide was much larger (5–7 times increase over starting pressure). These data show that high-voltage induced desorption is similar to thermal-induced desorption but with increased contributions of carbon derivatives.

The RGA was also used to monitor the conditioning process of the electrostatic deflector[8] of the Chalk River superconducting cyclotron. The deflector uses a 35 cm×2.5 cm negative high-voltage electrode at a gap of 5 mm from the septum and 1–2 cm from other grounded surfaces. It was conditioned, in 5 kV increments, from about 40 to 80 kV after it was repolished and rebuilt. Each increase in voltage beyond 40 kV produced large quantities of desorbed gas for about 1 min with a spectrum similar to that shown in Figs. 16 and 17. The quantity and composition of the desorbed gas did not change substantially whether the conditioning time was a few hours per increment or (as in two trials) after conditioning at a fixed voltage overnight and increasing the voltage after about 20 h.

F. The source of the desorption products

The mechanism of storage and release of large quantities of gas is an underlying problem of vacuum outgassing and the release of these products under the influence of increasing high voltage may provide some insight into the process. The estimate of about 10^{12} molecules per microdischarge gives some clue to a possible source of the desorption. If a microdischarge is, in fact, an avalanche discharge, it must originate from a small pocket of gas or liquid, likely trapped at a grain boundary or other imperfection in the metal. If each microdischarge of about 10^{12} molecules were from a spherical volume of gas trapped at one atmosphere, the diameter of the sphere would be about 40 μm. Features this large are never observed on a well-polished metal surface. If, however, each microdischarge originated from water or alcohol, trapped as liquid at atmospheric pressure, the diameter of a spherical volume equivalent to 10^{12} molecules is about 4 μm. This suggests that liquid may remain adsorbed on or near a metal surface, likely with an oxide layer or metal film over it. Careful optical microscopic examination of the micropolished metal surfaces used in these experiments revealed typically 50–200 pits/mm^2, with diameters of about 1–10 μm. While this may appear to be a large quantity, it represents about 0.1% of the total area of the metal surfaces which were polished to near mirror finish.

A series of experiments were performed to study the adsorption and desorption of water and ethanol using 304 stainless steel and oxygen-free copper. In the first experiments, the 1.9 cm diameter stainless-steel tube used for the experiments reported in Table I was heated, in vacuum, to about 530 °C without an electrode installed, cooled by flowing air on the atmospheric side and the test stand was vented to helium. The stainless-steel tube was quickly removed, subjected to a variety of treatments, repumped in less than 2 min and reheated after 30 min of pumping with a base pressure of about 2×10^{-7} Torr. Figure 18 shows results of this measurement. The x axis shows the time after the heater was turned on. Typical temperatures are shown near the top of the figure. The heat was turned off after 9 min and air cooling was used to return the temperature to about 25 °C by 14 min. The y axis shows the pressure increase over the background. Trial 1 shows the results of exposing the 14 cm long tube to air for 2 min, trial 2 the results of immersing the tube 5 cm into distilled water, and trial 3 the results of immersing the tube 5 cm into ethanol. The tube was blown dry by a pressurized nitrogen flow. The pumping speed of the test

stand for these measurements was measured as 60 l/s. The integral of pressure (Torr)×time(12 min×60 s)×pumping speed (60 l/s) was 0.54, 0.86, and 0.84 mTorr l for an area of about 45 cm^2 that was immersed in liquid in trials 2 and 3. This corresponds to $5-7\times10^{14}$ molecules/cm^2, less than a monolayer. Trial 4 shows the results of polishing about 5 cm of the tube with #600 aluminum oxide paper wetted with water, immersing the 5 cm region into an ultrasonic bath with detergent and rinsing in water and ethanol, i.e., a typical polishing procedure. The integral for this trial is 10.4 mTorr l or about 9×10^{15} molecules/cm^2. Trial 5 shows the results of the same polishing procedure, followed by pumping for 48 h before the thermal cycle. The amount of material desorbed is a substantial fraction of that in trial 4, indicating that the material is strongly bound. It is also noted that the surface finish of the stainless-steel tube was similar for all five trials and the apparent surface area should be the same.

The same tests were completed with a newly machined oxygen-free copper rod. The copper rod was about 15 cm long, 2.5 cm diameter at the heated end and stepped down to 1.5 cm diameter from the center of the rod to the end that was brazed to a stainless-steel vacuum flange. The final machining and polishing were done after the brazing. Because of the high thermal conductivity of copper, the temperature varied from 450 °C at one end to about 50 °C at the water-cooled flange. There were about 7×10^{16} molecules/cm^2 desorbed from the total surface during the initial thermal cycle to about 450 °C at the heated end. The copper desorbed about 3×10^{15} molecules/cm^2 after being dipped 5 cm into water or alcohol and about ten times more when polished with wetted #600 aluminum oxide abrasive during subsequent thermal cycles to 450 °C.

These experiments demonstrate that the machined or polished metal can store much more than monolayers of material, depending on the surface treatment. Another series of experiments were designed to show that this large quantity of material may be stored in discrete regions rather than uniformly over the entire surface of the metal. In these experiments, a micropolished copper electrode was used as a cathode at -50 kV with a gap of 6 mm, in the same geometry shown in Fig. 9. The anode was mounted on the thin-walled stainless steel tube used for thermal desorption experiments. Micropolished anodes of copper, stainless steel, niobium, and titanium were heated to about 550 °C while a sensitive detector was used to monitor x-ray activity between the electrodes. It was speculated that pockets of material adsorbed at high density would desorb in bursts and produce an avalanche discharge and x-rays. The x-ray detector was a Geiger counter that viewed the electrodes through the glass window, at a distance of about 14 cm from the anode. For these experiments, the detector efficiency was measured with a calibrated ^{241}Am source, temporarily placed between the electrodes. This source produces 59 keV gamma rays, somewhat higher than x rays produced by the 50 kV electrons used for these experiments. The source of 1×10^5 photons per second

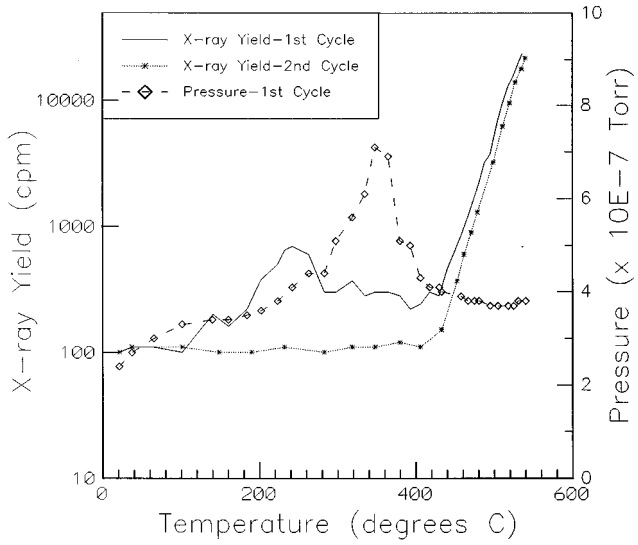

FIG. 19. The x-ray yield at 50 kV and the test stand pressure as a niobium anode is heated to 550 °C. The solid line shows the x-ray yield (referenced to the left-hand y axis) during the first thermal cycle. The coarse dashed line and data show the pressure, (referenced to the right-hand y axis). The fine dashed line and data show the x-ray yield during a second thermal cycle taken one day later, in which the electrode was reheated without venting the test stand. The pressure rise below 500 °C during the second cycle (not shown) was about 15% of the pressure increase during the first thermal cycle.

produced a yield of 100 counts/minute (cpm) above a background of about 100 cpm.

Figure 19 shows results from this experiment with a niobium anode. The data for the other electrodes were qualitatively similar. The x axis shows the temperature of the electrode. The solid line shows the x-ray yield as a micropolished anode was heated the first time after pumpdown. There was significant x-ray yield above a background of 80–100 cpm in the temperature range above about 150 °C, returning to a reduced yield between 300 and 440 °C and then increasing exponentially above 450 °C. The right-hand y axis shows the pressure in the test stand during the first thermal cycle. The dashed line (second cycle, left-hand y axis) shows the x-ray yield when the same electrode was reheated, without venting the test stand. There was no x-ray production (above background) and only a small (less than 15% compared to the first cycle) pressure rise for temperatures below 450 °C.

This figure demonstrates two different physical processes that were sorted out by additional experiments. The increased x-ray production below 450 °C is consistent with the picture of gas desorbing as high-density bursts from the anode as the temperature is increased. In order to produce x-rays, electrons must be produced and accelerated through some or all of the voltage across the gap. Electrons can be produced in this geometry from several sources: field emission from the cathode; an avalanche discharge in the volume between the electrodes producing electrons and ions; or from the release of positive ions from the heated anode that bombard the cathode, producing secondary electrons. It was un-

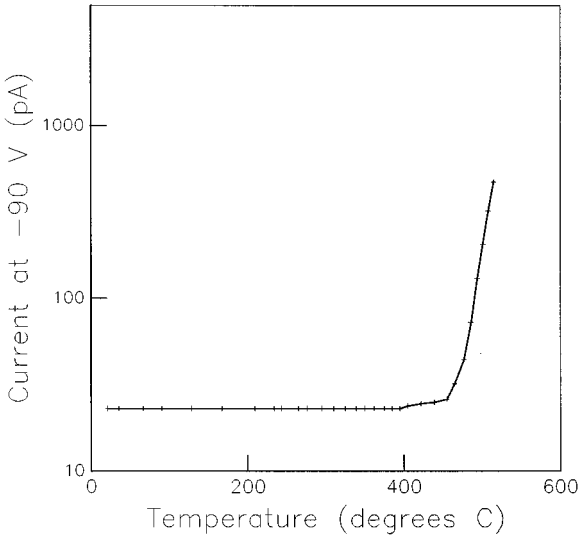

FIG. 20. The current measured with a 90 V battery in series with a picoampmeter connected to the cathode as a repolished niobium anode was heated through the same thermal cycle as in Fig. 19. The pressure rise (not shown) was similar to that shown in Fig. 19.

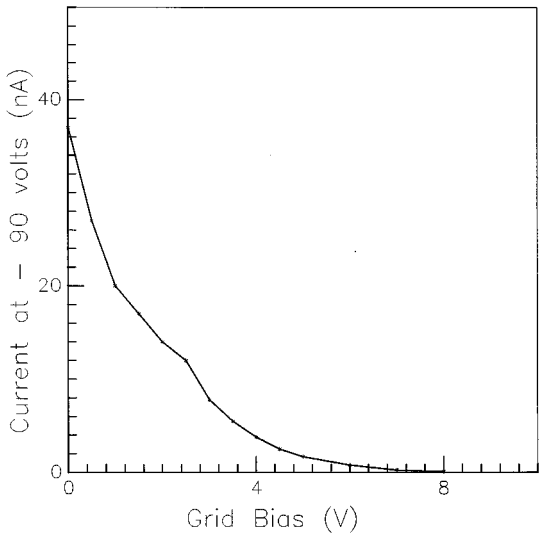

FIG. 21. The current measured with a picoampmeter in series with a 90 V battery connected to the cathode. A stainless-steel electrode was held at about 550 °C while the bias voltage was varied, as shown, on a fine grid about 1 mm in front of the heated electrode.

likely that the x-rays were produced by field emission because the field was low. There was also no indication of increased x-ray activity during the second thermal cycle (below 450 °C) which would subject the cathode to the same thermal load. Therefore, the x-ray yield below 450 °C could have been produced by an avalanche discharge in the gas, released in bursts from the heated anode. Experiments were then performed in which the cathode was connected to a 90 V battery in series with a picoammeter and a repolished niobium anode was heated through the same thermal cycle as in Fig. 19. Figure 20 shows the results from this. There was approximately 22 pA of background current, likely conducted along the dichromium trioxide on the insulator.[8] There was no current increase until 450 °C and then the current increased with the same slope shown by the exponentially increasing x-ray yield in Fig. 19. There was no measurable current change corresponding to the x-ray peak below 450 °C although the current sensitivity of the measurement was sufficient that the x-ray yield near 250 °C (see Fig. 19) would have produced an easily observable change if it were from current flowing across the gap producing secondary electrons at the cathode during the high-voltage measurement. There is not sufficient field at 90 V to produce gas multiplication and hence an avalanche discharge would not be possible.

The increased x-ray production at temperatures above 450 °C is likely due to a different phycsical process than is responsible for the increased yield at lower temperatures. The data of Fig. 20 clearly shows that there is current across the gap at the higher temperatures. To test if this was positive ion current, experiments were then conducted in which a thin (0.1 mm) grid with about 60% transmission and 0.5 mm grid spacing was placed about 2 mm in front of the cold anode surface. This distance was reduced to near-contact as the stainless-steel tube expanded while it was heated to 600 °C. Figure 21 shows the current measured with a picoampmeter in series with a 90 V battery connected to the cathode versus the bias on the grid. The stainless-steel electrode was maintained about 550 °C while the grid bias was changed as shown. The observations shown in Fig. 20 are consistent with positive ions leaving the heated surface. The current is unlikely to be electrons from the cathode because there are no significant changes occurring at that surface. This does not, however, rule out such possibilities as microparticles being ejected from the heated anode that cross the gap and release electrons from the cathode. The biased grid would not stop microparticles but may intercept the returning electrons. The observation of current from a heated anode surface is a recent finding in this program but this phenomena has been reported previously,[15,16] although there was no solid explanation of the physical processes that produced the current. There have been experiments in this program to determine if the observed current was correlated with a particular outgassing product and there was a strong correlation with molecular hydrogen desorption. The current was not affected by large (factor of 100 increase) changes in the test stand pressure. It was present for all metal electrodes tested as well as for stainless-steel and tungsten filaments. It was present when the electrodes were reheated several times during experiments similar to that reported in Fig. 20. However, when a thin (0.25 mm) diameter tungsten filament was heated the current persisted for only a few minutes at a given temperature. The current was not present when the thin tungsten filament was reheated for second and subsequent times.

IV. DISCUSSION

The experiments reported in this article provide strong evidence that gas is desorbed from the surface of a pair of

unconditioned metal electrodes subjected to increasing high voltage. The quantity released is large—equal to many monolayers—and the rate of release is often greater than 10^{-5} Torr ℓ/s cm^2–i.e., several orders of magnitude greater than vacuum outgassing at room temperature. Both the composition and quantity desorbed are similar to that produced through thermal-induced desorption of the same metals. Some key observations about microdischarges are:

(1) Each microdischarge is correlated with a burst of desorbed gas and some current across the high voltage gap.
(2) Once microdischarges are triggered, they cover the whole area of the electrodes.
(3) Over periods of tens of seconds to many minutes at a fixed voltage, microdischarge activity ceases.
(4) Microdischarge activity is retriggered with a small (few percent) increase in high voltage.
(5) The anode is the main precursor of activity.
(6) For gaps of millimeters to a few centimeters, microdischarge activity is more dependent on the total voltage than the electric field.

There is also evidence of a close correlation between microdischarge activity and vacuum outgassing. High-voltage-induced desorption, i.e., microdischarge activity, efficiently removes gas from a metal surface while thermal desorption of an anode greatly reduces microdischarge activity.

These observations lead to questions about the physical processes that occur, the most important issues being: the inception of the process and its dependence on high voltage; the source of the gas and the link between vacuum high-voltage insulation, and outgassing. These are considered below.

A. Inception of voltage-induced desorption and the dependence on voltage

The physical processes that lead to voltage-induced desorption of gas have been extensively investigated without a successful resolution. The key questions that remain unanswered are how does an increasing voltage trigger the process and why is the process dependent on the total voltage rather than the electric field. The anode is the main precursor of the activity and if one examines physical processes that occur at the anode, there are few that could produce the observations. The most likely is that electrons with an intensity below the level of detection sensitivity of these experiments are the precursor. Electrons have a range of a few μm at 30 kV for the metal electrodes used in these experiments, increasing by nearly a factor of 10 at 100 kV. This range is of the same magnitude as the diameter of the regions of trapped liquid water that have been postulated as the source of the large quantity of material stored near the surface of a machined or polished metal. If one assumes that the microdischarges are from bursts of liquid trapped near the surface, it is instructive to calculate the energy required to produce an explosive burst and the quantity of electrons required to produce this energy. From the thermal-induced desorption shown in Fig. 15, the peak of the water desorption is at about 250 °C. At this temperature, the local pressure of liquid water would be about 50 atmospheres. If all of the energy of 50 kV electrons were deposited in a 4 μm diameter sphere of water, it would require about 10^6 electrons (less than 1 pC) to increase the temperature by 250 °C. The total quantity of charge transferred per microdischarge eventually reaches about 10^{10} electrons or ions (see Sec. III A 2), much larger than required to initiate the process by this method. Typical ions such as oxygen or nitrogen have a range of less than 0.1 μm in metals such as copper, but they will produce secondary electrons with a yield greater than unity per incident ion[17] when they impact the cathode. Once ionization is initiated, this secondary production can be part of a regenerative buildup. The large difference between the ranges of ions and electrons may be the reason that the desorption process is initiated in unconditioned anodes (see Figs. 7 and 8) and not unconditioned cathodes. It is noted that the rise time of a microdischarge is greater than 50 μs (see Fig. 2) and there may be a much longer time of regenerative buildup preceding this in which there is not sufficient detection sensitivity to measure the activity. This is enough time for many transits of ions and electrons. What are possible sources of electrons? Although field-emitted electrons have not been observed before microdischarge activity, they may be present at a level below detection sensitivity of these experiments. Measurements have been reported[18] that used microchannel plates to observe field-emitted electrons at currents between 10^{-18} and 10^{-14} A, well below the sensitivities of these experiments. However, field emission tends to be limited to a few localized sites on a cathode. The intensity of field-emitted electron current increases exponentially with increasing field. These are different than the observed dependence of microdischarges with changing field and voltage. It may be that the initial electrons are from random ionization in the gap as was proposed[4] earlier. Some process would then be needed to enhance the small initial number of electrons. The buildup process of microdischarges has many characteristics of the electrical buildup in a Geiger counter.[19] In that instrument, the initial ionization produces electrons that are accelerated to the central anode wire. The strong field at the anode produces multiplication in the counter gas at a pressures of about 0.1 atmosphere. The gas multiplication then spreads rapidly along the anode wire. There are many asperities on both electrode surfaces that produce substantial field peaking. It may be in these regions that an initial ionization breaks up trapped hydrocarbons to produce the initial volume of gas to start the regenerative process. The RGA spectra show enhanced quantities of hydrogen and light hydrocarbons compared to thermally induced desorption of the same metal electrodes prepared in the same manner. The hydrocarbons may originate from residual pump oils that are adsorbed on the electrode surfaces. While there is some consistency between these ideas and the observations, it is recognized that this is quite speculative.

B. Source of the gas

The experiments described in Sec. III F give strong evidence of the large quantity of material that can be stored in a

polished metal surface. Figure 18 shows that polishing a metal surface that had been previously degassed at high temperature increases the quantity of material readsorbed by more than an order of magnitude compared to just immersing the metal in water, alcohol, or air. There are at least two possibilities for the large differences in the quantity of gas adsorbed in these two situations. The polishing procedure may force water deep into pores with an oxide film over regions of high density or the abrasive may remove an oxide layer that permits much stronger adsorption. There is also evidence (Figs. 19 and 20) that the material may be stored at high density such as a liquid. This may be a significant aspect of vacuum outgassing.

The polishing process may well increase the amount of material driven into a metal surface even compared to initial machining. No experiments were done that made a direct comparison of desorption from a newly machined surface compared to a well-polished surface. However, experiments have demonstrated a large increase in the high-voltage insulation capability of well-polished surfaces compared to machined metal surfaces. This is an important practical aspect of this research.

C. Connection between gas desorption and high-voltage insulation

This article has demonstrated that one of the main components of high-voltage conditioning is the desorption of gas as the voltage is increased. It is also possible that explosive bursts at the anode propel microparticles to the cathode that serve as a source of field emission. A companion article[6] has shown that very high fields can be reached without any measurable field emission. This has been achieved by careful polishing of the electrodes and the vacuum chamber that they are used in. Conditioning processes that recognize the importance of gas desorption have been implemented. These included conditioning the anode and cathode with separate power supplies (one at a time) to the maximum supply voltage, often using conditioning periods of several hours per few kV increment at the higher voltages. One of the electrodes is mounted on a moveable insulator and high-voltage feedthrough. The conditioning to the maximum total voltage is done at a wider gap, and then the gap is closed and the conditioning repeated. Conditioning at a wider gap desorbs the gas with less likelihood of a spark that may lead to field emission. These procedures have resulted in many demonstrations of high fields with no measurable field emission. The highest fields without field emission have been obtained by heating both electrodes to about 700 °C in a separate vacuum oven, cooling, wiping the cathode surface with ethanol during the transfer to the test stand and quickly transferring the anode without wiping it.

It is the belief of the author that weakly bound particles on the walls of the vacuum chamber are often transferred to the cathode, resulting in field emission. Once field emission is present electrical breakdown is usually determined by thermal stability of the anode. The field-emitted electron beam is focused to a small spot on the anode producing a high power density. Once temperatures exceeding about 500 °C are reached at a local region of the anode, an exponentially increasing source of current is produced as demonstrated in Figs. 19 and 20. This is positive feedback that can rapidly lead to breakdown. Depending upon the physical processes that lead to the positive ion production, it may be that part of the high-voltage conditioning process, once field emission is present, is to deplete the source of positive ions, permitting higher temperatures to be reached at the anode. There is evidence of this in the operation of the electrostatic deflector of the Chalk River superconducting cyclotron. Field-emitted electrons are focused by the strong magnetic field (up to 5 T) and some evaporation of the stainless steel anode surfaces occurs without destructive breakdowns. However, if field emission can be avoided or at least kept quite low, it is possible to operate a practical high-voltage device for long periods. The cyclotron deflector has been operated for more than 2000 h during the past year, often at fields of up to 15 MV/m (75 kV over a gap of 5 mm), usually with no measurable field emission. The superconducting cyclotron presents a particularly harsh environment[8] for operation of a high-voltage device because of the strong magnetic field, high residual rf fields and a dirty environment. All of the lessons learned from the experimental program—such as careful preparation of all surfaces, careful conditioning procedures and the use of water cooling of the high-voltage electrode—have been applied to this successful demonstration of high-voltage technology.

V. CONCLUSIONS

The experiments reported in this article demonstrated that large quantities of gas were desorbed from unconditioned metal electrodes as the voltage was increased between them. This is one of the most important aspects of high-voltage conditioning, especially for large (greater than a few mm) gaps. These experiments also showed the close link between high-voltage-induced gas desorption and vacuum outgassing. The gas was often released in bursts of 50–500 μs pulse length with sufficient density (about 10^{12} molecules per pulse) to sustain an avalanche discharge during the burst. The gas was released under the influence of increasing voltage, with much less dependence on field.

Physical processes that lead to the storage and release of gas are suggested. The dependence on voltage rather than field is difficult to reconcile. However, once the desorption process is initiated, higher voltages will lead to more energetic ions and electrons with greater depth of penetration. At this time, investigations have already shown: the gas composition was similar to thermal-induced outgassing with higher concentrations of carbon-based products; the total quantity of gas released was comparable to that released from heating the electrode to about 500 °C in vacuum; there was evidence, from several different experimental approaches, that the gas originated from regions of high density stored on or near the surface of the metal; and that positive ions were produced from a metal surface heated above 500 °C. These ions likely

serve as part of a feedback process that produces electrical breakdown at high voltage.

The author has attempted to present his interpretation of this complex behavior but is well aware that there may be others. It is noted that the data presented in this and a companion[6] article represent a small but illustrative sample of the total data. There were many repeats of the key experimental results and other experiments were conducted to assist in reaching the present understanding of the data. The experiments have been described in sufficient detail that they can repeated by others and it is hoped that the results presented will stimulate further work along these lines.

The observations reported in this article lead to a different view of adsorption of material into a metal surface, and of the vacuum outgassing process itself. This may provide new insight into the processes that affect the use of metals in a vacuum system for other uses. Finally, the material presented here and in the companion article[6] presents a very different picture of the complex process of vacuum high-voltage insulation from that previously held.

[1]H. P. S. Powell and P. A. Chatterton, Vacuum **20**, 419 (1970).
[2]G. Munzenberg, W. Faust, S. Hofmann, H. J. Schott, and K. Guttner, Nucl. Instrum. Methods **166**, 391 (1979).
[3]R. Hawley, A. A. Zaky, and M. E. Zein Eldine, Proc. IEEE **112**, 1237 (1965).
[4]P. A. Chatterton, *Electrical Breakdown of Gases*, edited by M. Meek and J. D. Craggs (Wiley, New York, 1978), Chap. 2, pp. 129–208.
[5]D. Alpert, D. A. Lee, E. M. Lyman, and H. E. Tomaschke, J. Vac. Sci. Technol. **1**, 35 (1964).
[6]W. T. Diamond, J. Vac. Sci. Technol A. **16**, 707 (1998).
[7]W. T. Diamond, G. R. Mitchel, J. Almeida, and H. Schmeing, in Proceedings of the 1991 IEEE Particle Acceleration Conference, San Francisco, California, 1991 (unpublished), p. 979.
[8]W. T. Diamond, C. R. Hoffmann, G. R. Mitchel, and H. Schmeing, Proceedings of 13th International Conference on Cyclotrons and their Applications, Vancouver, 1992 (unpublished), p. 569.
[9]W. T. Diamond, Proceedings of the 1993 IEEE Particle Acceleration Conference, Washington, D.C., 1993 (unpublished), p. 1381.
[10]P. A. Redhead, J. P. Hobson, and E. V. Kornelsen, *The Physical Basis of Ultrahigh Vacuum* (Chapman and Hall, London, 1968).
[11]M. Li and H. F. Dylla, J. Vac. Sci. Technol. A **12**, 1772 (1994).
[12]S. Rezaie-Serej and R. A. Outlaw, J. Vac. Sci. Technol. A **12**, 2814 (1994).
[13]P. K. Sharma and G. S. Hickey, J. Vac. Sci. Technol. A **12**, 867 (1994).
[14]N. W. Robinson, *The Physical Principles of Ultra-High Vacuum* (Chapman and Hall, London, 1968), Chap. 7.
[15]D. G. Samaras, *Theory of Ion Flow Dynamics*, Prentice-Hall International Series in Space Technology (Prentice-Hall, New Jersey, 1962), p. 204.
[16]A. von Engel, *Ionized Gases*, 2nd ed. (Oxford University Press, Great Britain, 1965), p. 89.
[17]G. Carter and J. S. Colligon, *Ion Bombardment of Solids* (Heinemann, London, 1968), Chap. 3.
[18]H. Isono, A. Kojima, M. Sone, and H. Mitsui, Proceedings of the XIVth International Conference on Discharges and Electrical Insulation, Santa Fe, New Mexico, 1990 (unpublished), p. 122.
[19]A. P. Arya, *Fundamentals of Nuclear Physics* (Allyn and Bacon, Boston, MA, 1966), p. 51.